Selenoprotein H is an essential regulator of redox homeostasis that cooperates with p53 in development and tumorigenesis

Andrew G. Cox[a], Allison Tsomides[a], Andrew J. Kim[a], Diane Saunders[a], Katie L. Hwang[a], Kimberley J. Evason[b], Jerry Heidel[c], Kristin K. Brown[d], Min Yuan[d], Evan C. Lien[d], Byung Cheon Lee[a,e], Sahar Nissim[a], Bryan Dickinson[f], Sagar Chhangawala[g], Christopher J. Chang[h,i], John M. Asara[d], Yariv Houvras[g], Vadim N. Gladyshev[a,j], and Wolfram Goessling[a,j,k,l,1]

[a]Brigham and Women's Hospital, Harvard Medical School, Boston, MA 02115; [b]University of Utah, Salt Lake City, UT 84112; [c]Oregon State University, Corvallis, OR 97331; [d]Beth Israel Deaconess Medical Center, Harvard Medical School, Boston, MA 02115; [e]Korea University, 02841 Seoul, Republic of Korea; [f]University of Chicago, Chicago, IL 60637; [g]Weill Cornell Medical College and New York Presbyterian Hospital, New York, NY 10065; [h]Howard Hughes Medical Institute, Bethesda, MD 20815; [i]University of California, Berkeley, CA 20815; [j]Broad Institute of MIT and Harvard, Cambridge, MA 02142; [k]Harvard Stem Cell Institute, Cambridge, MA 02138; and [l]Dana-Farber Cancer Institute, Harvard Medical School, Boston, MA 02115

Edited by Leonard I. Zon, Howard Hughes Medical Institute, Boston Children's Hospital, Harvard Medical School, Boston, MA, and accepted by Editorial Board Member Carol Prives July 18, 2016 (received for review January 7, 2016)

Selenium, an essential micronutrient known for its cancer prevention properties, is incorporated into a class of selenocysteine-containing proteins (selenoproteins). Selenoprotein H (SepH) is a recently identified nucleolar oxidoreductase whose function is not well understood. Here we report that *seph* is an essential gene regulating organ development in zebrafish. Metabolite profiling by targeted LC-MS/MS demonstrated that SepH deficiency impairs redox balance by reducing the levels of ascorbate and methionine, while increasing methionine sulfoxide. Transcriptome analysis revealed that SepH deficiency induces an inflammatory response and activates the p53 pathway. Consequently, loss of *seph* renders larvae susceptible to oxidative stress and DNA damage. Finally, we demonstrate that *seph* interacts with p53 deficiency in adulthood to accelerate gastrointestinal tumor development. Overall, our findings establish that *seph* regulates redox homeostasis and suppresses DNA damage. We hypothesize that SepH deficiency may contribute to the increased cancer risk observed in cohorts with low selenium levels.

selenium | selenoproteins | p53 | liver cancer | endoderm development

Selenium is an essential micronutrient that has been implicated in cancer chemoprevention and is thought to delay the severity of cardiovascular and neurologic disorders (1). The biological properties of selenium are mediated by a diverse group of selenocysteine (Sec)-containing selenoproteins (2). Sec is incorporated into protein in response to the UGA opal codon in a unique context in which the 3′ UTR of the gene contains a Sec insertion sequence (SECIS) element (3, 4). The human selenoproteome includes five glutathione peroxidases (GPX1-4, 6), three thioredoxin reductases (TXNRD1-3), and one methionine sulfoxide reductase (MSRB1) that act in concert to provide antioxidant defense (2). The selenoproteome also includes three iodothyronine deiodinases (DIO1-3) that control thyroid hormone metabolism and two selenoproteins that are involved in selenoprotein synthesis (SPS2) and transport (SELP). In contrast, little is known regarding the function of the other 11 human selenoproteins (SELW, SELT, SELH, SELV, SELI, SEP15, SELM, SELK, SELS, SELO, and SELN) (5).

Although selenium was originally considered a toxin, classic work by Schwartz and Foltz showed that selenium prevents liver necrosis in rats, suggesting that it is an essential micronutrient (6). This essential role as a micronutrient during development was subsequently recognized by the livestock industry and is now widely known for human health (7). Genetic disruption of three mammalian selenoproteins–GPX4, TXNRD1, and TXNRD2–causes embryonic lethality (8–12) in murine models. SelP-deficient mice exhibit impaired selenium transport from the liver to peripheral tissues and show growth retardation and impaired motor coordination (13, 14). In contrast, mice deficient in Gpx1 (15), Gpx2 (16), Gpx3 (17), MsrB1 (18), Sep15 (19), or SelM (20) are viable, with more subtle defects, some of which only manifest in the context of stress.

Epidemiologic surveys have shown that selenium deficiency may be associated with an increased risk of certain types of cancer (21, 22). For example, patients with cirrhosis (scarring) of the liver have a high risk of developing liver cancer, and are typically deficient in selenium (23–26). However, selenium supplementation chemoprevention trials have provided mixed results, possibly related to a combination of unknown baseline selenium status and genetic factors that modulate selenoprotein function (22). In vivo cancer studies using transgenic mice have revealed that the role of selenoproteins in tumorigenesis is context-dependent, both preventing and promoting cancer (27, 28). The importance of

Significance

Dietary selenium and selenoproteins play important roles in regulating redox processes that impact human health. The human genome includes 25 genes for selenoproteins, which have diverse roles in redox homeostasis, thyroid hormone metabolism, endoplasmic reticulum quality control, selenium transport, and other functions. Selenoprotein H (*seph*) is a recently identified nucleolar oxidoreductase with DNA-binding properties whose function is not well understood. In this work, we used a unique combination of unbiased metabolomic and transcriptomic approaches in zebrafish to discover that *seph* is an essential regulator of redox homeostasis that regulates p53. In addition, we demonstrate the *seph*-deficient adults are prone to chemically induced carcinogenesis. Our results suggest that *seph* suppresses oxidative stress and DNA damage in the nucleolus.

Author contributions: A.G.C. and W.G. designed research; A.G.C., A.T., A.J.K., D.S., K.L.H., K.J.E., J.H., K.K.B., M.Y., E.C.L., B.C.L., and S.N. performed research; B.D. and C.J.C. contributed new reagents/analytic tools; A.G.C., A.T., K.J.E., J.H., K.K.B., M.Y., E.C.L., S.C., J.M.A., Y.H., V.N.G., and W.G. analyzed data; C.J.C., J.M.A., Y.H., and V.N.G. provided general input on study design and analysis; and A.G.C. and W.G. wrote the paper.

The authors declare no conflict of interest.

This article is a PNAS Direct Submission. L.I.Z. is a Guest Editor invited by the Editorial Board.

Data deposition: The data reported in this paper have been deposited in the Gene Expression Omnibus (GEO) database, www.ncbi.nlm.nih.gov/geo (accession no. GSE85943).

[1]To whom correspondence should be addressed. Email: wgoessling@partners.org.

This article contains supporting information online at www.pnas.org/lookup/suppl/doi:10.1073/pnas.1600204113/-/DCSupplemental.

selenium and selenoproteins in embryonic development and tumorigenesis underscores the need for a better understanding of the biological function of the recently identified selenoproteins.

Here we show that *seph* (ortholog of human *SELH*) plays an essential role in vertebrate organ development. Using unbiased metabolomic and transcriptomic approaches, we found that SepH deficiency alters redox homeostasis, provokes an inflammatory response, and activates p53. SepH-deficient zebrafish larvae exhibit an increased susceptibility to oxidative stress and DNA damage. Loss of p53 partially mitigates the developmental defects observed in *seph* mutants; however, loss of p53 function combines with SepH haploinsufficiency in adulthood to accelerate gastrointestinal (GI) tumor development. Collectively, our results establish that SepH regulates redox homeostasis and suppresses DNA damage during development and tumorigenesis.

Results

***seph* Mutant Zebrafish Exhibit Defects in Organ Development.** This investigation was spurred by the isolation of a *seph* mutant from a large-scale insertional mutagenesis screen (29). This *seph* mutant was caused not by viral insertion into the coding region, but rather by insertion into the 3′ UTR. Sequence analysis indicated that the virus is inserted in the 3′ UTR upstream of the regulatory SECIS element (Fig. 1 and Fig. S1*A*); therefore, we infer that loss of function in *seph* mutants is caused by displacement of the SECIS element and a consequent inability to read the in-frame UGA codon as Sec. We found that *seph* expression, present in the head region of wild type (WT) embryos, was completely absent in the *seph* mutant larvae at 3 dpf (Fig. S1*B*). This is consistent with previous studies demonstrating that *SELH* (human ortholog of *seph*) is among the most sensitive selenoprotein mRNAs to changes in abundance in response to selenium status, owing to the differences in Sec incorporation efficiency and nonsense-mediated decay (30, 31).

Developmental defects in homozygous *seph* mutants begin to manifest morphologically by 3 d postfertilization (dpf), and the mutants lose viability by 12–14 dpf (Fig. 1*B*). At 5 dpf, *seph* mutants exhibit craniofacial defects with smaller eyes (microphthalmia), impaired yolk absorption, and an uninflated swim bladder (Fig. 1*C*). To examine the effect of SepH deficiency on endodermal organ development, we imaged *seph* mutants on transgenic reporter fish, highlighting the liver and exocrine pancreas [*Tg(ela3l:GFP;fabp10a:dsRed)*] at 5 dpf, which revealed dramatically impaired liver and pancreas development (Fig. 1*C*). Quantification of liver and pancreas fluorescence revealed that the *seph* mutant liver was ∼40% smaller than WT liver, whereas the pancreas was almost absent (Fig. 1 *D* and *E*). Similarly, we assessed organ development in *Tg(gata6:GFP)*, which highlights endodermal organs, and *Tg(fabp2:dsRed)*, which illuminates the intestinal epithelium of larvae, and this confirmed that *seph* mutants exhibit defects in intestinal development (Fig. S1 *C* and *D*).

To confirm that the loss of *seph* gene function induced by disruption of the SECIS element is responsible for the developmental defects, we injected an antisense morpholino targeting *seph* into WT embryos at the one-cell stage, which resulted in a morphant phenotype that recapitulates the *seph* mutant (Fig. S1*E*). Whole-mount in situ hybridization (WISH) analysis for *fabp10a*, *trypsin*, and *fabp2* expression in *seph* morphants and mutants compared with WT larvae at 72 hpf revealed that *seph* plays a critical role in liver, pancreas, and gut formation (Fig. S1 *E* and *F*). To verify that loss of *seph* is responsible for the mutant phenotype, we performed a rescue experiment injecting *seph* mutant embryos with mRNA encoding GFP-labeled murine selenoprotein h (*selh*). We found that expression of either N- or C-terminal SelH-GFP fusion constructs (GFP-SelH^{Sec38Cys} or

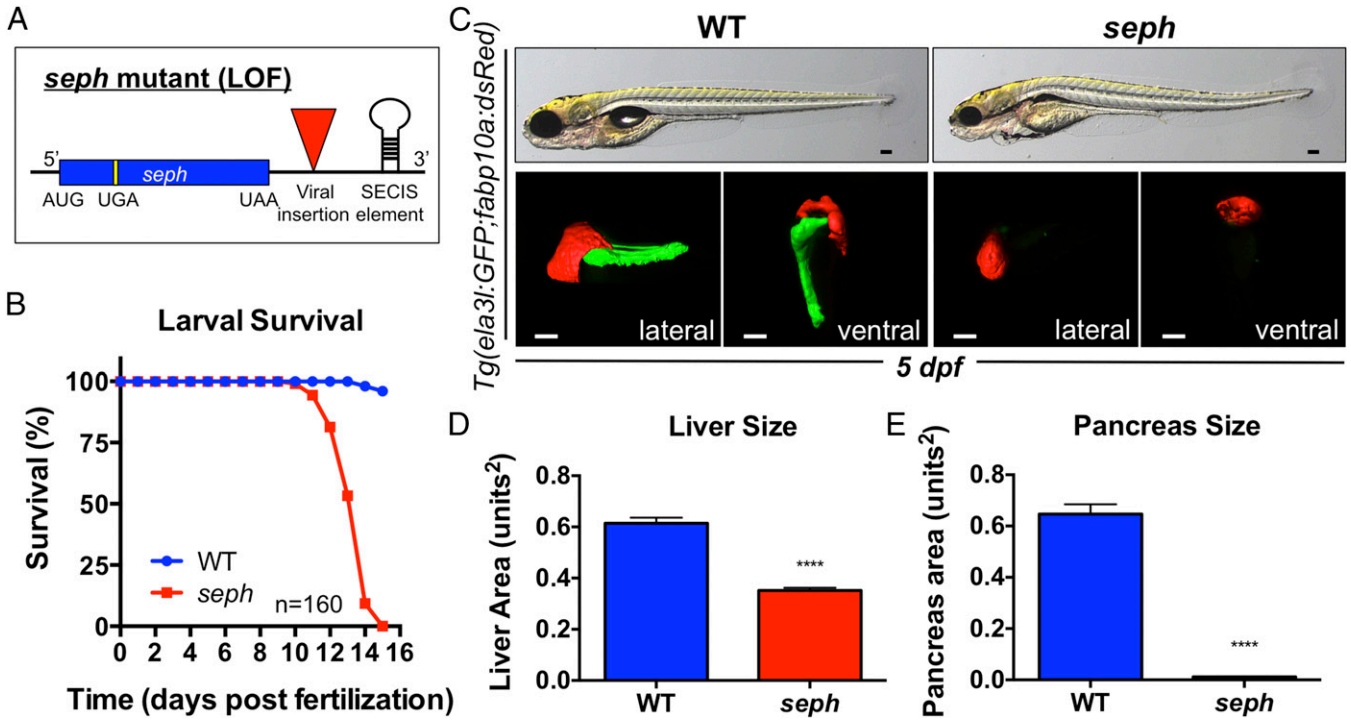

Fig. 1. *seph* mutant zebrafish exhibit defects in organ development. (*A*) Schematic illustrating the nature of the *seph* mutant. (*B*) Survival of WT and homozygous *seph* mutant larvae over time. $n = 160$ larvae. (*C*) Morphological assessment and fluorescent imaging (lateral and ventral views) of WT and *seph* mutant larvae on a Tg(*ela3l:GFP;fabp10a:dsRed*) background by confocal tomography at 5 dpf. Liver volume: WT, 3.09e^6 μm^3; *seph*, 1.69e^6 μm^3. Pancreas volume: WT, 2.79e^6 μm^3; *seph*, undetectable. (Scale bar: 100 μm.) (*D*) Quantitative analysis of fluorescent liver area in WT and *seph* mutant larvae at 5 dpf. $n = 16$. ****$P < 0.0001$. (*E*) Quantitative analysis of fluorescent pancreas area in WT and *seph* mutant larvae at 5 dpf. $n = 16$. ****$P < 0.0001$.

SelH^{Sec38Cys}-GFP) (32, 33) was sufficient to rescue the *seph* mutant phenotype in the vast majority of injected embryos (Fig. S1 *G* and *H*). Taken together, these experiments demonstrate that *seph* is an essential gene that plays a key role in endodermal organ development.

Metabolomic Characterization of *seph* Mutant Larvae Reveals That SepH Modulates Redox Homeostasis. Given the central role of many selenoproteins in oxidative metabolism, we aimed to characterize the metabolic status of *seph* mutant larvae. Polar metabolites were extracted from WT and homozygous *seph* mutant larvae at 5 dpf and analyzed by targeted LC-MS/MS via selected reaction monitoring (SRM) (34). Hierarchical clustering based on metabolite abundance showed significant changes in steady-state levels of a small fraction of the metabolites that were enriched (fold enrichment represents the normalized number of metabolites overrepresented from a predefined metabolic pathway) in the urea cycle, pyrimidine biosynthesis, and methionine (Met) metabolism (Fig. 2 *A* and *B*). No significant changes in the abundance of reduced or oxidized glutathione were observed (Fig. S2*A*). *seph* mutants had reduced NAD$^+$:NADH and NADP$^+$:NADPH ratios, due in most part to the large reductions in the abundance of NAD$^+$ and NADP$^+$, respectively (Fig. 2*C* and Fig. S2*B*). Interestingly, the *seph* mutants showed a reduction in Met levels and a concomitant increase in the abundance of Met sulfoxide (MetSO) (Fig. 2*D*). Consequently, the Met:MetSO redox status was substantially disrupted in the *seph* mutant larvae (Fig. 2*E*). Furthermore, *seph* mutants exhibited a dramatic reduction in the abundance of the antioxidant ascorbic acid (vitamin C) (Fig. 2*F*). Given the imbalance of the Met:MetSO redox state, we measured MetSO reductase (Msr) activity (both MsrA and MsrB) in larval lysates. These analyses showed no difference between WT and *seph* mutants (Fig. S2*C*), suggesting elevated Met oxidation in the mutant. Collectively, these studies illustrate that SepH plays an important role in maintaining specific aspects of redox homeostasis related to ascorbate and Met metabolism.

SepH-Deficient Larvae Are Prone to Oxidative Stress. To further assess the role of SepH in regulating reactive oxygen species during development, we visualized H_2O_2 generation in vivo using the boronate-based H_2O_2 probe, PF2. PF2 fluorescence was increased in homozygous *seph* mutant larvae at 5 dpf (Fig. 3 *A* and *B*). Fluorescence intensity was heterogeneous in distribution, but most apparent in the endodermal and head regions. *seph* mutants were extremely sensitive to menadione-induced oxidative stress, resulting in axis curvature and global edema (Fig. 3 *C* and *D*). Taken together, these studies demonstrate that *seph* mutants have impaired antioxidant defense.

Transcriptomic Profiling Reveals That SepH Deficiency Provokes an Inflammatory Response and Activates the p53 Pathway. To determine whether SepH deficiency causes a transcriptional response that contributes to the developmental phenotype, we performed global RNAseq on WT and homozygous *seph* mutant larvae at 5 dpf. Transcriptomic profiling of differentially expressed genes revealed that SepH deficiency causes widespread changes in gene expression (Fig. 4*A* and Fig. S3*A*). Transcriptome profiling also further determined the extent of organ defects, including severe reductions in endoderm/hepatic progenitors (*sox17*, *prox1*) and hepatic (*fabp10a*), intestinal (*fabp2*), and pancreatic (*trypsin*) transcripts, with no changes in kidney (*cdh17*)- or vessel (*kdrl*)-related transcripts (Fig. S3*B*). Supporting the metabolic data indicating defects in Met metabolism, Gene Set Enrichment Analysis (GSEA) identified that *seph* mutants express a gene set associated with Met deprivation (Fig. S3*C*). Interestingly, GSEA also revealed that SepH deficiency enhances the expression of inflammatory response genes, including *tnfa*, *il-1b*, *il-11a*, *socs3b*, and *lifrb* (Fig. 4 *B* and *C* and Fig. S3*D*). *seph* mutants also demonstrated a strong induction of p53 target genes, including *tp53*, *mdm2*, *ccng1*, and *rps27l* (Fig. 4*D* and Fig. S3*E*). The results of our transcriptome analysis support the idea that loss of SepH provokes an inflammatory response and activates the p53 pathway.

SepH-Deficient Larvae Are Sensitive to DNA Damage. Having observed that SepH deficiency activates a transcriptional p53 response, we tested whether p53 activation contributes to the developmental

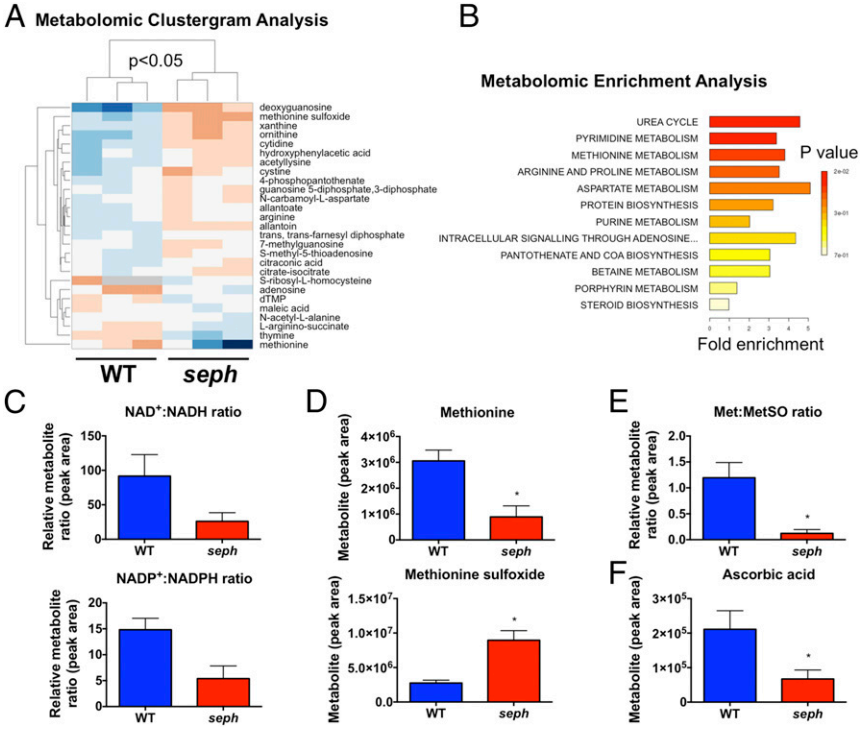

Fig. 2. Metabolomics reveals that SepH deficiency modulates redox homeostasis. (*A*) Clustergram analysis of polar metabolite abundance in WT and *seph* mutant larvae at 5 dpf as determined by LC-MS/MS via SRM analysis. $n = 3$. $P < 0.05$. (*B*) Metabolite set enrichment of polar metabolites in WT and *seph* mutant larvae as determined by SRM analysis. (*C*) Steady-state ratio of redox-related metabolites NAD$^+$:NADH, and NADP$^+$:NADPH in WT and *seph* mutant larvae at 5 dpf. (*D*) Steady-state abundance of Met (reduced) and MetSO (oxidized) in WT and *seph* mutant larvae at 5 dpf. $n = 3$. $^*P < 0.05$. (*E*) Met:MetSO ratio in WT and *seph* mutant larvae at 5 dpf. $n = 3$. $^*P < 0.05$. (*F*) Steady-state abundance of ascorbic acid in WT and *seph* mutant larvae at 5 dpf. $n = 3$. $^*P < 0.05$.

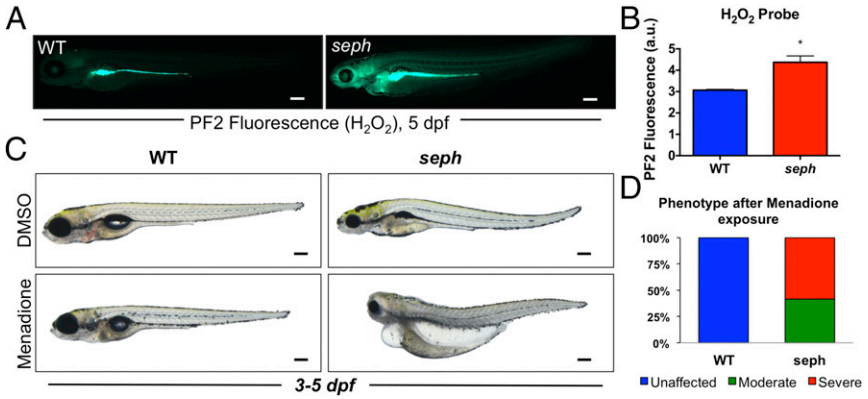

Fig. 3. SepH deficient larvae are prone to oxidative stress. (*A*) Fluorescent detection of H_2O_2 (PF2 fluorescence) in WT and *seph* mutant larvae at 5 dpf. (Scale bar: 200 μm.) (*B*) Quantification of H_2O_2 in WT and *seph* mutant larvae at 5 dpf. $n = 5$. $^{**}P < 0.01$. (*C*) Morphological assessment of WT and *seph* mutant larvae exposed to menadione (1 μM) from 3 to 5 dpf. (Scale bar: 200 μm.) (*D*) Quantification of phenotype (unaffected, moderate, or severe) observed following menadione (1 μM) exposure from 3 to 5 dpf. Moderately affected larvae include minor defects, such as edema and tail curling, whereas severely affected larvae include major defects, such as widespread tissue necrosis (loss of transparency).

phenotype. Immunoblot analysis demonstrated dramatically elevated p53 levels in *seph* mutant larvae (Fig. 5*A*). To examine whether the cell cycle is affected, we performed whole-mount immunohistochemistry probing bromo-deoxyuridine (BrdU) incorporation, and found that *seph* mutants incorporate lower levels of BrdU (Fig. S4*A*). Consistent with cell cycle defects, FACS analysis demonstrated that *seph* mutants exhibit an increased number of cells in the G0 phase and a decreased number of cells in the S or G2/M phase (Fig. S4*B*).

We next examined the response of *seph* mutants to DNA damage after exposure to UV irradiation (200 J/m^2) and found that they were highly sensitized compared with WT larvae, with 50% mortality at 2 d postexposure (dpe) (Fig. 5*B*). Consistent with this notion, SepH-deficient larvae also were very sensitive to exposure to the DNA-damaging agent camptothecin (1 μM), with an 80% drop in survival at 2 dpe (Fig. 5*C*). Taken together, these studies reveal that *seph* mutant larvae exhibit cell cycle defects and are prone to DNA-damaging agents.

Given the involvement of p53 in the defects observed in *seph* mutant larvae, we tested whether the *seph* mutant phenotype persists in the absence of p53. Crossing *seph* mutants onto a *tp53*^{M214K} mutant background partially rescued the *seph* mutant phenotype. At the gene expression level, the loss of p53 in *tp53;seph* compound mutant larvae suppresses activation of p53 target genes *rps27l* and *mdm2*; however, we still observed activation of inflammatory genes, such as *tnfa* and *il11a* (Fig. S4*C*). At the morphological level, the craniofacial, eye, and endodermal organ defects were less severe in *tp53;seph* compound mutant larvae compared with *seph* mutants (Fig. 5*D*). Deeper examination by WISH analysis demonstrated that the loss of p53 rescued liver and, to a lesser effect, gut development in *tp53;seph* compound mutant larvae, but had no effect on exocrine pancreas development (Fig. 5*E* and Fig. S4*D*).

To examine the brain defects, we determined the expression of the neuron-specific gene *elavl3* by WISH and quantitative PCR (qPCR) and observed a dramatic reduction in *seph* mutants compared with WT larvae, and this reduction was not altered in *tp53;seph* compound mutant larvae (Fig. S5 *A* and *B*). Minor defects in cartilage development also were apparent in both seph and *tp53;seph* compound mutant larvae at 5 dpf (Fig. S5*A*). Histological analysis revealed that *seph* mutants exhibit hepatocyte ballooning and signs of cell death, which are markedly reduced in *tp53;seph* compound mutant larvae at 5 dpf (Fig. 5*D*). Further immunohistochemical analysis of the *seph* mutants established that cell proliferation (PCNA) in the liver is decreased concomitant with an increase in apoptosis (cleaved caspase-3), and that these effects are partially rescued in the *tp53;seph* compound mutant larvae (Fig. S5 *C* and *D*). Taken together, these studies reveal that loss of *tp53* partially mitigates the developmental defects observed in *seph* mutant larvae.

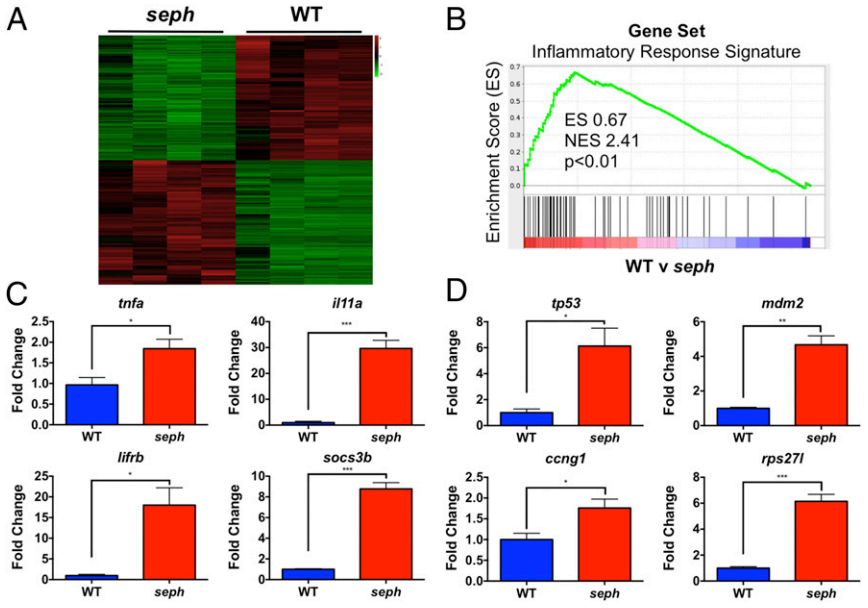

Fig. 4. Transcriptomic profiling reveals that SepH deficiency provokes an inflammatory response and activates the p53 pathway. (*A*) Heatmap of statistically significant differential gene expression as determined by RNAseq between WT and *seph* mutant larvae at 5 dpf. $n = 4$. $P < 0.05$. (*B*) GSEA showing that the SepH deficiency is highly enriched in genes associated with an inflammatory response signature. ES, 0.67; NES, 2.41. $P < 0.05$. (*C*) qPCR expression analysis of specific genes associated with an inflammatory response (*tnfa*, *il11a*, *socs3b*, and *lifrb*) in WT and *seph* mutant larvae at 5 dpf. $n = 3$. $^{*}P < 0.05$; $^{***}P < 0.001$. (*D*) qPCR expression analysis of specific genes associated with p53 activation (*mdm2*, *ccng1*, *tp53*, and *rps27l*) in WT and *seph* mutant larvae at 5 dpf. $n = 3$. $^{*}P < 0.05$; $^{**}P < 0.01$; $^{***}P < 0.001$.

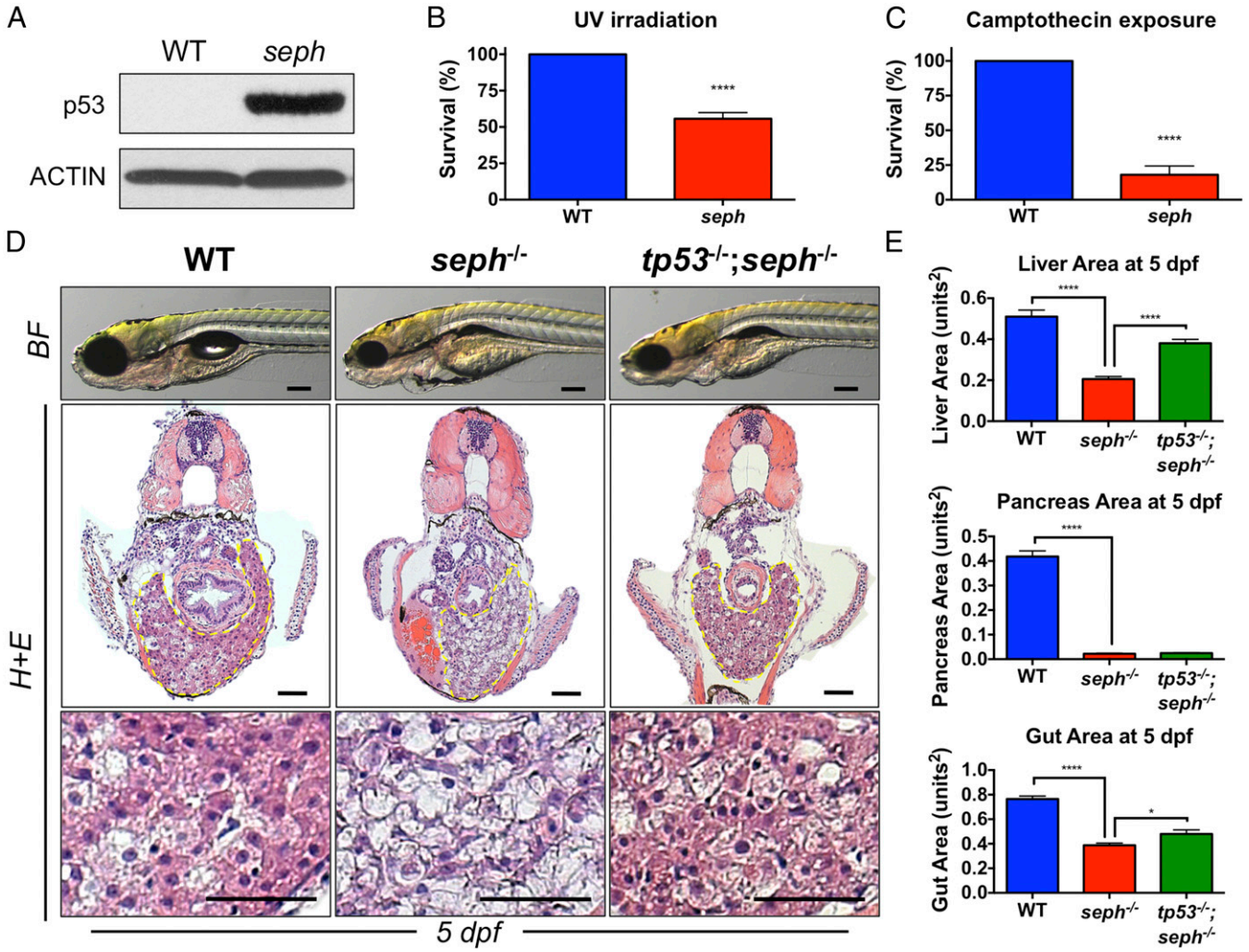

Fig. 5. *seph* mutants are sensitive to DNA damage. (*A*) Immunoblot analysis of p53 expression in WT and *seph* mutant larvae at 5 dpf. (*B*) Survival of WT and *seph* mutant larvae 2 dpe to UV irradiation (200 J/m^2, 7 dpf). $n = 7$. ****$P < 0.0001$. (*C*) Survival of WT and *seph* mutant larvae 2 dpe to camptothecin (1 μM). $n = 10$. ****$P < 0.0001$. (*D*) Morphological and histological analysis of WT, *seph*$^{-/-}$ and *tp53*$^{-/-}$;*seph*$^{-/-}$ mutant larvae at 5 dpf. The yellow dashed region represents the liver. The region of histology showing the larval liver is shown in the zoomed images. [Scale bars: 200 μm (brightfield; BF) and 50 μm (histology; H+E).] (*E*) Quantitative analysis of liver, pancreas, and gut area in WT, *seph*$^{-/-}$, and *tp53*$^{-/-}$;*seph*$^{-/-}$ mutant larvae at 5 dpf. $n > 8$. *$P < 0.05$; ****$P < 0.0001$.

***seph* Genetically Interacts with p53 Deficiency to Accelerate GI Tumor Formation.** Having shown that SepH deficiency disrupts redox homeostasis, provokes an inflammatory response, and activates p53 in development, we next examined whether SepH plays an important role in suppressing tumor development. We exposed progeny of *tp53*$^{-/-}$;*seph*$^{+/-}$ fish to the carcinogen dimethylbenzanthracene (DMBA) at 3 wk postfertilization and followed tumor development in the fish over a period of 1 y (Fig. 6*A*). In our analysis, we focused on GI tumor development, which became readily apparent because GI tumor-bearing fish have distended abdomens and on dissection reveal tumors that can be confirmed histologically and segregated by genotype (Fig. 6*B*). We analyzed GI tumor-free survival in this cohort of fish and found that SepH deficiency (heterozygous mutant) significantly accelerated tumor onset (Fig. 6*C*). By the end of the 1-y investigation, 29 of 58 (50%) *tp53*$^{-/-}$;*seph*$^{+/-}$ fish harbored tumors, compared with 5 of 23 (22%) p53$^{-/-}$ fish ($P = 0.0344$). Histological analysis of the tumors that developed identified 52% of the *tp53*$^{-/-}$;*seph*$^{+/-}$ tumors as being of hepatic origin and 28% as being of pancreatic origin (Fig. 6*D*). Most of the liver tumors were hepatocellular carcinomas (HCCs) (Fig. S6*A*), whereas the majority of the pancreatic tumors were pancreatic acinar cell carcinomas (PACCs) (Fig. 6*E* and Fig. S6*B*). Here 21% of the tumors in the *tp53*$^{-/-}$;*seph*$^{+/-}$ fish and 20% of the tumors in the *tp53*$^{-/-}$ fish were malignant spindle cell neoplasms, most likely representing either malignant mixed neoplasms of the intestine and/or malignant peripheral nerve sheath tumors (MPNSTs) (Fig. 6*E* and Fig. S6*C*). Taken together, these studies show that loss of *seph* synergizes with loss of *tp53* and the carcinogen DMBA in promoting carcinogenesis.

Discussion

The micronutrient selenium plays an essential role in human health, and its effects are mediated by incorporation, in the form of the 21st amino acid Sec, into 25 proteins that compose the human selenoproteome. Despite the extensive functional information for some members of the selenoproteome, such as thioredoxin reductases, glutathione peroxidases, thyroid hormone deodinases, and MetSO reductases, relatively little is known about several more recently identified selenoproteins, which has spurred inquiry into their biological functions (2). SepH is one such protein of unknown function, which is conserved in vertebrates, and its functional homologs are present across metazoa. Because of this conservation, zebrafish represent a particularly

attractive model for examining SepH functions. In this study, we found that *seph* mutants exhibited impaired organ development and failed to survive into adulthood. *seph* mutants were susceptible to oxidative stress and showed defects in maintaining the redox state of Met and ascorbate. *seph* mutant larvae exhibited a sustained inflammatory response and activation of p53, which contributed to the embryonic phenotype. *seph*-haploinsufficient adult fish were more prone to developing GI tumors. Collectively, these studies identify unique aspects of SepH function in regulating organ development and tumorigenesis by maintaining redox homeostasis and suppressing DNA damage (Fig. S7). In light of these studies, we hypothesize that SepH deficiency is an important factor contributing to human pathophysiology associated with selenium deficiency.

Biological Features of SepH. SepH is a recently identified 14-kDa thioredoxin fold-like protein with a conserved CXXU motif (5). Initial biochemical studies have shown that SepH is a nucleolus-localized oxidoreductase with glutathione peroxidase activity and a DNA-binding AT hook domain (32, 33). In vitro studies have shown that selenium depletion significantly decreases *seph* mRNA abundance (35), whereas selenite exposure up-regulates *seph* mRNA abundance (36). Selenium status tightly regulates *seph* mRNA abundance in mice to a greater extent than most other selenoproteins (37); for example, a selenium-deficient diet was found to cause a 60% reduction in *seph* mRNA abundance in murine liver, kidney, intestine, and splenic leukocytes owing to nonsense-mediated decay (37–40). Recent elegant studies reported by the Hatfield and Howard laboratories used ribosome profiling to reveal that dietary selenium differentially regulates selenoprotein expression in the liver, with *gpx1*, *sepw1*, and *seph* being the most sensitive to dietary selenium (30). In vivo expression studies in zebrafish have shown that *seph* mRNA is localized to proliferative zones of the central nervous system and brachial arches over the first 2 dpf (41). Parallel studies examining the *Drosophila* homolog of *seph*, known as BthD, have shown that the protein is expressed in the salivary gland during embryogenesis and in the adult ovary (42). Taken together, these studies highlight the integral role of selenium in regulating SepH abundance.

No studies of genetic SepH deficiency in vertebrate models have been reported to date, and the majority of the functional studies examining the biological role of SepH have been performed in cell culture. Overexpression of SEPH in cultured cells up-regulates enzymes associated with de novo glutathione synthesis, providing resistance to glutathione depletion (33). In a similar manner, SEPH overexpression protects cells from ultraviolet b (UV-B) irradiation by suppressing p53 activation (43, 44). At the molecular level, up-regulation of SEPH triggers an AKT-PKA-CREB pathway that culminates in the activation of PGC1α and NRF1, which stimulates mitochondrial biogenesis, leading to enhanced oxygen consumption and respiration (44–46). Conversely, knockdown of SEPH expression renders cancer cells

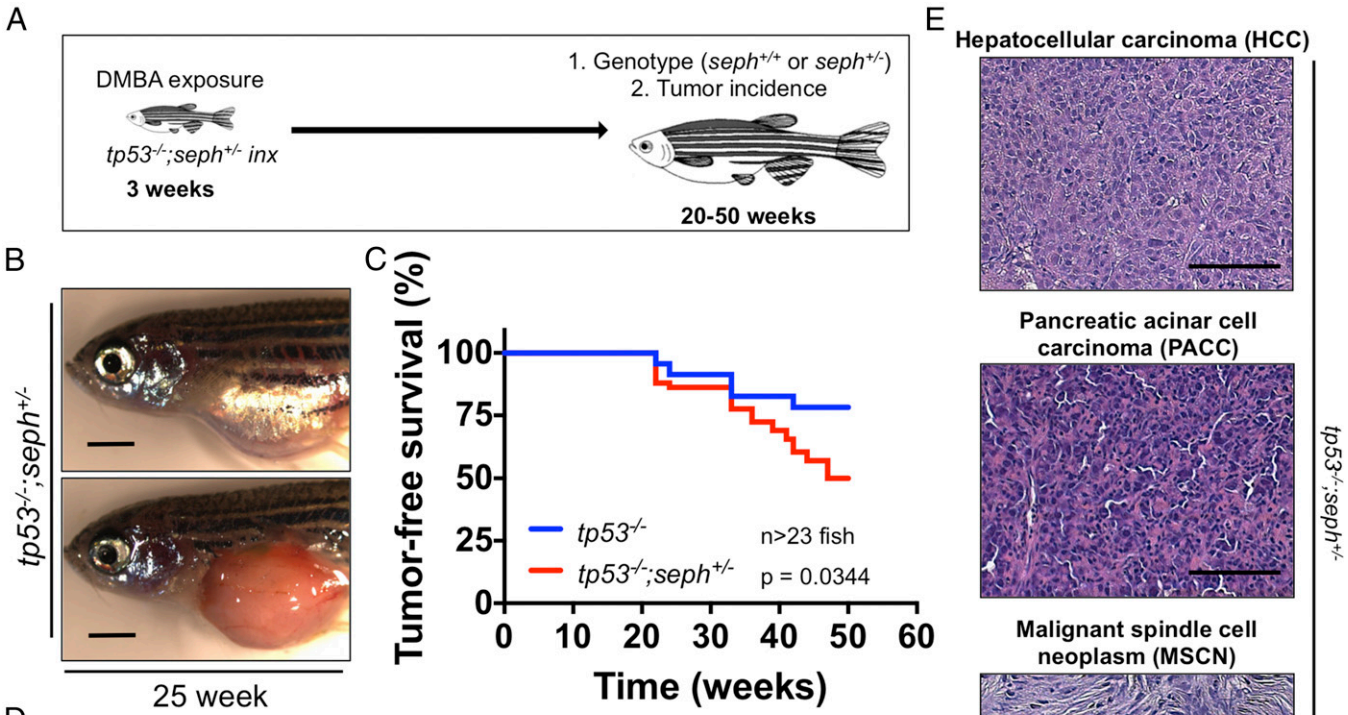

D

Fish Line	Pancreatic Cancer	Liver Cancer	Intestinal Cancer	Malignant Spindle Cell Neoplasm
***tp53*$^{-/-}$**	40% (2/5)	40% (2/5)	0% (0/5)	20% (1/5)
***tp53*$^{-/-}$*;seph*$^{+/-}$**	28% (8/29)	52% (15/29)	10% (3/29)	21% (6/29)

Fig. 6. *seph* genetically interacts with p53 deficiency to accelerate GI tumor formation. (*A*) Scheme illustrating the protocol used to study DMBA-induced tumorigenesis. (*B*) Example of a GI tumor in a *tp53*$^{-/-}$;*seph*$^{+/-}$ fish exposed to DMBA. (Scale bar: 2 mm.) (*C*) Kaplan–Meier analysis of Tumor-free survival in *tp53*$^{-/-}$ and *tp53*$^{-/-}$;*seph*$^{+/-}$ fish exposed to DMBA. $n > 25$ fish. $P = 0.0344$, Mantel–Cox log-rank test. (*D*) The incidence of pancreatic cancer, liver cancer, intestinal cancer, and malignant spindle cell neoplasm in *tp53*$^{-/-}$ and *tp53*$^{-/-}$;*seph*$^{+/-}$ fish exposed to DMBA. (*E*) Histological evaluation of GI tumors identified in *tp53*$^{-/-}$;*seph*$^{+/-}$ fish showing examples of PACC, HCC, and malignant spindle cell neoplasm (MSCN). (Scale bar: 100 μm.)

susceptible to H_2O_2 (32). Recent work by Wu et al. (47) showed that *SEPH* knockdown causes oxidative stress, which inhibits proliferation and induces senescence in fibroblasts. In that study, the authors found that H_2O_2 exposure in SEPH-deficient cells provoked a sustained DNA damage response and senescence, which was inhibited by loss of ATM or p53 function. In our present study, we have defined the mechanism of SepH function in vivo and discovered that it regulates redox homeostasis and integrates a DNA damage response involving p53, which culminates in organ defects during development and a susceptibility to tumorigenesis in adulthood.

The Nucleolus as a Stress Sensor. Our findings demonstrate that deficiency of the nucleolar protein SepH provokes an inflammatory stress response and activates p53. Recent studies support the emerging concept that the nucleolus acts as a stress sensor facilitating p53 activation (48). Previous studies have proposed the thought-provoking hypothesis that the diverse stimuli known to activate p53 share the ability to disrupt nucleoli; these studies show that DNA damage is not sufficient to activate p53, but instead that p53 activation depends on nucleolar disruption (49, 50). A number of nucleolar proteins, including PICT (51), RPL5 (52), RPL6 (53), RPL11 (54-56), RPL23 (57), RPL26 (58, 59), RPS6 (60), RPS7 (61, 62), RPS27L (63), NPM (64–66), and NCL (58, 59), regulate the MDM2-p53 pathway. Recent studies have shown that the 5S ribonucleoprotein particle (RNP), comprising RPL5, RNP11, and 5S rRNA, regulates p53 on ribosomal stress (67–69). Elegant studies using *rps27l* mutant mice have provided evidence that RPS27L regulates p53-suppressing genomic instability and tumorigenesis (63). In the present study, we have demonstrated that SepH deficiency leads to the induction of *rps27l*, consistent with nucleoli disruption. Consequently, our work further illuminates previous studies by providing evidence that SepH acts as a redox sensor that integrates oxidative stress to the nucleolar stress response pathway.

Zebrafish Models of Ribosomal and Nucleolar Stress. Zebrafish has proven to be a useful model in which to examine the effect of ribosomal biogenesis and nucleolar stress in vivo. Zebrafish have been used to model several ribosomopathies, including Diamond–Blackfan anemia (DBA), dyskeratosis congenital (DC), and Shwachman–Bodian–Diamond syndrome (SBDS). Studies have shown that loss of *rps19* (70–74), *rps24* (75), *rps29* (76), *rpl11* (77–79), and *rpl22* (80) lead to hematopoietic defects reminiscent of DBA. In many cases, the DNA damage response contributes to p53 activation in zebrafish models of DBA (71). Defects in genes linked to DC, such as *nop10*, lead to a p53-dependent loss of hematopoietic stem cells (81). The gene responsible for SBDS, which regulates ribosomal biogenesis, plays an essential role in pancreas development (82). Furthermore, ribosomal proteins are often enriched in endodermal organs, and many are required for pancreas development (83). For example, the nucleolar protein Nom1 plays a critical role in ribosomal biogenesis and pancreas development (84). The ribosomal biogenesis factors Bms1 and Wdr43 cause tissue-specific defects in endodermal and neural crest development, respectively (85, 86). Heath et al. (87) recently reported that loss of a critical component of the small subunit processome, *pw2h*, causes defects in ribosome biogenesis, leading to impaired organ development and induction of autophagy as a survival response. Groundbreaking work by Amsterdam et al. (88) has revealed that many genes encoding components of the ribosome act as haploinsufficient tumor suppressors in zebrafish. Follow-up studies have revealed that the MPNSTs that form from a loss of ribosomal genes exhibit a loss of p53 expression and are highly aneuploid (89–91). Recent work by Provost et al. (92) showed that ribosomal gene *rpl36* restrains $Kras^{G12V}$-induced pancreatic cancer. Our study provides a different angle on the field by establishing a nucleolus-localized selenoprotein, SepH, which plays a critical role in regulating the nucleolar stress response in development and cancer. Taken together, these studies highlight the advantages of zebrafish as a model system for studying ribosome and nucleolar biology in the context of development and cancer.

Selenoproteins Play Essential Roles in Tissue Homeostasis and Cancer. Our findings provide evidence that SepH exhibits a tumor-suppressor function in the context of carcinogen-induced tumorigenesis. The tumor-suppressive activity of SepH is consistent with its role in regulating redox homeostasis, inflammation, and DNA damage during embryonic development. SepH deficiency collaborates with a loss of p53 function to accelerate GI tumorigenesis. Interestingly, we found that SepH-deficient fish exhibited induction of inflammatory genes, such as *tnfa* and *il11a*, even in the absence of p53. Given the recently reported tumor-promoting effects of *tnfa* (93, 94) and *il11* (95, 96), we suspect that inflammation plays an important role in SepH-deficient tumors. The spectrum of tumors that we observed in the SepH-deficient fish included PACC, HCC, cholangiocarcinoma, intestinal cancer, and malignant spindle cell neoplasms, which resemble the MPNSTs that arise spontaneously in $tp53^{M214K}$ mutant zebrafish (97).

Previous studies using Sec transfer RNA (tRNA) (*trsp*)-deficient mice have greatly increased our understanding of selenoprotein function. Germline disruption of *trsp* in mice leads to early embryonic lethality (98). Tissue-specific loss of *trsp* in endothelial cells, skin cells, osteochondroprogenitor cells, or neurons leads to a panoply of defects that share such features as growth retardation, degeneration, and premature death (99–103). Liver-specific loss of *trsp* disrupts selenoprotein synthesis and causes liver necrosis and death (104). Selenoprotein deficiency in the liver activates the hepatoprotective Nrf2 response and increases susceptibility to diethylnitrosamine (DEN)-induced tumorigenesis (101, 105, 106). Similarly, hematopoietic-specific loss of selenoproteins leads to oxidative stress, hemolytic anemia, and sustained activation of Nrf2 (107, 108). Prostate-specific *trsp* KO mice exhibit prostate neoplasia, demonstrating that selenoproteins function as tumor suppressors in the murine prostate (109, 110). In a comparable manner, mammary gland- specific loss of *trsp* renders mice susceptible to DMBA-induced tumorigenesis (111).

Gpx1/2 double-KO mice exhibit bacteria-induced inflammation (colitis) that spontaneously drives intestinal tumor formation (112, 113). Gpx2 appears to play a complex role in colon carcinogenesis (114), where it inhibits inflammation-driven tumorigenesis (115), yet promotes growth of xenografted tumors (116). Loss of GPX2 leads to dedifferentiation of cells to a progenitor-like state (117). Conversely, overexpression of GPX2 leads to cell differentiation, with increased proliferation and tumor-forming potential (117). Selenium status has a complex role in mouse models of cancer, as demonstrated by studies showing that both selenium deficiency and selenium supplementation can reduce the tumor incidence in different mouse models (118, 119). Taken together, these studies shed light on the complexity of the relationship between selenium status and tumorigenesis, while emphasizing the essential function of selenoproteins in maintaining tissue homeostasis and suppressing tumorigenesis.

In conclusion, we have demonstrated that SepH regulates redox homeostasis and plays an essential role in organ development and tumor suppression. Given the potency by which SepH is regulated by selenium intake, we propose that SepH deficiency contributes to the deleterious phenotypes associated with selenium deficiency.

Experimental Procedures

Zebrafish Husbandry. Zebrafish were maintained according to Harvard Medical School Institutional Animal Care and Use Committee, protocol #04626. The following lines were used in this study: WT (AB), $seph^{hi2737Tg}$ (*seph* mutant), $tp53^{zdf1}$ ($p53^{M214K}$, loss of function) Tg(*ela3l:EGFP;fabp10a:dsRed*)^{gz15},

Tg(*gata6:GFP*)^{ae5}, and Tg(*fabp2:dsRed*)^{zf129}, as described previously (29, 97, 120–123).

Chemical Exposure. Zebrafish larvae were exposed to menadione (1 μM), camptothecin (1 μM), and DMBA (5 ppm), as described above. When necessary, chemicals were dissolved in DMSO. Unless indicated otherwise, all chemicals were obtained from Cayman Chemicals or Sigma-Aldrich.

Morpholino Injection. Morpholinos (GeneTools; PhiloMath) designed against the ATG and site of SepH (5′- CGAGTCGCCATTGCAGCAGCAACAA-3′) or scrambled controls were injected into AB embryos at the one-cell stage.

mRNA Rescue Experiment. SelH-GFP mRNA was synthesized using previously described SelH^{Sec38Cys}-GFP or GFP-SelH^{Sec38Cys} mammalian expression constructs (32, 33) as templates in conjunction with primers containing a T7 promoter (GFP-SelH^{Sec38Cys}: forward primer, GGCTAATACGACTCACTATAGGATGGTGAGCAAGGGCGAGGA; reverse primer, GCTCTTTATGAAAGGTACTTCTTC; SelH^{Sec38Cys}-GFP: forward primer, GGCTAATACGACTCACTATAGCATGGCCCCCCACGGAAGAAAG; reverse primer, GCTTTACTTGTACAGCTCGTC). SelH^{Sec38Cys}-GFP or GFP-SelH^{Sec38Cys} mRNA was synthesized using the mMESSAGE mMACHINE T7 Kit (Ambion). GFP mRNA was synthesized using pCS2-GFP as a template with the mMESSAGE mMACHINE SP6 Transcription Kit (Ambion). Poly(A) tails were added to mRNA using the Poly(A) Tailing Kit (Ambion) according to the manufacturer's instructions. GFP, SelH^{Sec38Cys}-GFP, or GFP-SelH^{Sec38Cys} mRNA (100 ng/μL) was injected into *seph* mutant embryos (200 pg/egg) at the one-cell stage. GFP-positive embryos were sorted at 1 dpf, and larvae were imaged at 5 dpf. Individual larvae were subsequently genotyped using a three-primer multiplex assay (5′-GAGCAGTTTAACAGTTTAGCAGCTTAAC-3′, 5′-CCATTGTTCAGTTCTGCTGTCAC-3′, and 5′-CTGTTCCATCTGTTCCTGAC-3′), which gave a 172-bp band (WT) and a 240-bp band (*seph* transgenic).

Whole-mount In Situ Hybridization. Paraformaldehyde (PFA)-fixed larvae were processed for in situ hybridization according to standard zebrafish protocols (www.zfin.org). The following RNA probes were used: *seph*, *fabp10a*, *fabp2*, *trypsin*, and *elav3*. Expression patterns represent the average of >50 larvae per treatment. Alternatively, the area of staining was analyzed using Fiji as described previously (124).

Fluorescence Microscopy. Fluorescent liver and pancreas reporter [Tg(*ela3l:EGFP;fabp10a:dsRed*)^{gz15}], endoderm [Tg(*gata6:GFP*)^{ae5}], or intestinal reporter [Tg(*fabp2:dsRed*)^{zf129}] larvae were put under anesthesia with 0.04 mg/mL Tricaine-S, and microscopy was performed. Larvae were imaged using a Zeiss Discovery V8/AxioCam MRc with the Axiovision software suite. Lightsheet microscopy was performed using a Zeiss Lightsheet Z.1 at the Harvard Center for Biological Imaging core. Fluorescent images were analyzed using Fiji as described previously (124).

Steady-State Metabolomics Analysis. WT and *seph* mutant larvae were isolated at 5 dpf, and methanol extraction was performed. Polar metabolites were isolated and enriched using the methodology outlined by Yuan et al. (34). Metabolite fractions were collected and analyzed by targeted LC-MS/MS via SRM with positive/negative ion polarity switching using a QTRAP (quadrupole-linear ion trap) 5500 hybrid triple quadrupole mass spectrometer (AB Sciex).

RNA Transcriptomic Analysis. WT and *seph* mutant larvae were isolated at 5 dpf, and RNA was extracted with TRIzol (Life Technologies) according to the manufacturer's instructions. RNA quality was checked using an Agilent 2100 Bioanalyzer. Sequencing was performed after library construction on an Illumina HiSeq. polyA sequence data were annotated on the ZV9 genomic assembly to identify differentially affected genes (125). Gene Ontology and GSEA of biological processes were determined by GAGE (Gene Ontology Consortium) (126).

qRT-PCR. RNA was isolated from pooled zebrafish larvae using TRIzol. After DNase treatment, cDNA was synthesized using the SuperScript III First-Strand Synthesis Kit (Life Technologies). qRT-PCR was performed on biological triplicates using an iCycler with iQ SYBR Green (Bio-Rad). Gene expression was analyzed with *ef1a* as the reference gene (Table S1).

H_2O_2 Detection. H_2O_2 generation was examined in 5 dpf WT and *seph* mutant larvae by exposure to 5 μM peroxyfluor-2 (PF2) (127) for 1 h at 28 °C. After incubation, PF2-loaded larvae were washed, and fluorescence was imaged.

MSR Activity Assay. MsrA and MsrB activity was assayed from 5 dpf WT and *seph* mutant larval lysates (500 μg) as described previously (128). In brief, the reductions of dabsylated Met-*R*-SO and dabsylated Met-*S*-SO by lysates in the presence of NADPH were quantified by HPLC.

BrdU Incorporation Assay. Proliferation was assessed in zebrafish larvae using whole-mount immunohistochemistry to examine the incorporation of BrdU. Larvae were immersed in 200 μg/mL BrdU (B-5002; Sigma-Aldrich) for 4 h before fixation. Larvae were processed for whole-mount immunohistochemistry, probed with anti-BrdU (Roche; clone 9318), and visualized using HRP-conjugated secondary coupled with a 3,3′-diaminobenzidine (DAB) substrate kit.

DNA Content Analysis. The cell cycle was examined in disaggregated zebrafish larvae at 5 dpf by FACS analysis of DNA content. Larvae were disaggregated by mechanical disruption with a small pestle in a tube in 200 μL of PBS (10 larvae/tube). Cells were strained through a 35-μM nylon mesh, stained with 10 μg/mL Hoechst 33342, and incubated in the dark for 30 min before FACS analysis. DNA content (VioFL1) of individual cells defined the G0/G1 phase (n), the G2/M phase (2n), and the S phase (intermediate).

Alcian Blue Staining. PFA-fixed 5 dpf larvae were bleached in H_2O_2, stained in Alcian blue solution [1% HCl, 70% (vol/vol) ethanol, 0.1% Alcian blue] overnight, and rinsed in acidic ethanol.

Histology. PFA-fixed fish were paraffin-embedded, cut into serial sections, and stained with hematoxylin and eosin using standard techniques.

Immunohistochemistry. Fixed tissue embedded in paraffin was serially sectioned before immunohistochemical analysis. Slides were deparaffinized and rehydrated before heat-induced antigen retrieval. Antigens were detected using primary antibodies, such as anti-PCNA (Anaspec; AS-55421) and anti-cleaved caspase-3 (Abcam; ab13847), in conjunction with an HRP/DAB (ABC) detection kit (Abcam; ab64264) according to the manufacturer's instructions (R&D Systems).

Immunoblot Analysis. Larval extracts were prepared from 5 dpf WT and *seph* mutant larvae. Lysates were resolved by SDS/PAGE and transferred electrophoretically onto nitrocellulose. Membranes were probed with anti-p53 (Abcam; ab77813) or anti–β-actin (Cell Signaling Technology; 4967) overnight and then detected with secondary antibody conjugated with HRP. Antibody complexes were visualized by enhanced chemiluminescence using X-ray film.

DMBA-Induced Carcinogenesis. Here 3-wk-old p53$^{-/-}$ and p53$^{-/-}$;SepH$^{+/-}$ fry were exposed to DMBA dissolved in DMSO for 24 h, as described previously (129). The next day, the fry were rinsed several times in aquarium water before being returned to the aquarium tanks. Fish were monitored closely for gastrointestinal tumor development over the next 12 mo (excluding fish with ocular tumors). Fish with distended abdomens were dissected, and tumors were confirmed and diagnosed by histological analysis by two independent pathologists (K.J.E. and J.R.H.), who were blinded to the fish genotype.

ACKNOWLEDGMENTS. This work was supported by an Irwin Arias Postdoctoral Fellowship (to A.G.C.) and Liver Scholar Award (to A.G.C.) from the American Liver Foundation; Harvard Digestive Disease Center Pilot Feasibility Grant P30 DK034854 (to A.G.C.); and National Institutes of Health (NIH) Grants T32GM007753 (to K.L.H.), NCI 5K08CA172288 (to K.J.E.), R01 GM061603 (to V.N.G.), and R01 DK090311 and R24OD017870 (to W.G.). K.J.E. was a Robert Black Fellow supported by the Damon Runyon Cancer Research Foundation (DRG-109-10). C.J.C. is an Investigator with the Howard Hughes Medical Institute and has received support from NIH Grant GM 79465. J.M.A. is partially supported by NIH Grants 5P01CA120964 and 5P30CA006516. W.G. is supported by the Claudia Adams Barr Program for Innovative Cancer Research and is a Pew Scholar in the Biomedical Sciences.

1. Rayman MP (2012) Selenium and human health. *Lancet* 379(9822):1256–1268.
2. Labunskyy VM, Hatfield DL, Gladyshev VN (2014) Selenoproteins: Molecular pathways and physiological roles. *Physiol Rev* 94(3):739–777.
3. Berry MJ, et al. (1991) Recognition of UGA as a selenocysteine codon in type I deiodinase requires sequences in the 3′ untranslated region. *Nature* 353(6341):273–276.
4. Berry MJ, Banu L, Harney JW, Larsen PR (1993) Functional characterization of the eukaryotic SECIS elements which direct selenocysteine insertion at UGA codons. *EMBO J* 12(8):3315–3322.
5. Kryukov GV, et al. (2003) Characterization of mammalian selenoproteomes. *Science* 300(5624):1439–1443.

6. Schwarz K, Foltz CM (1958) Factor 3 activity of selenium compounds. *J Biol Chem* 233(1):245–251.
7. Black RE (2001) Micronutrients in pregnancy. *Br J Nutr* 85(Suppl 2):S193–S197.
8. Conrad M (2009) Transgenic mouse models for the vital selenoenzymes cytosolic thioredoxin reductase, mitochondrial thioredoxin reductase and glutathione peroxidase 4. *Biochim Biophys Acta* 1790(11):1575–1585.
9. Jakupoglu C, et al. (2005) Cytoplasmic thioredoxin reductase is essential for embryogenesis but dispensable for cardiac development. *Mol Cell Biol* 25(5):1980–1988.
10. Conrad M, et al. (2004) Essential role for mitochondrial thioredoxin reductase in hematopoiesis, heart development, and heart function. *Mol Cell Biol* 24(21): 9414–9423.
11. Yant LJ, et al. (2003) The selenoprotein GPX4 is essential for mouse development and protects from radiation and oxidative damage insults. *Free Radic Biol Med* 34(4): 496–502.
12. Imai H, et al. (2003) Early embryonic lethality caused by targeted disruption of the mouse PHGPx gene. *Biochem Biophys Res Commun* 305(2):278–286.
13. Hill KE, et al. (2003) Deletion of selenoprotein P alters distribution of selenium in the mouse. *J Biol Chem* 278(16):13640–13646.
14. Schomburg L, et al. (2003) Gene disruption discloses role of selenoprotein P in selenium delivery to target tissues. *Biochem J* 370(Pt 2):397–402.
15. Cheng WH, et al. (1997) Cellular glutathione peroxidase knockout mice express normal levels of selenium-dependent plasma and phospholipid hydroperoxide glutathione peroxidases in various tissues. *J Nutr* 127(8):1445–1450.
16. Esworthy RS, Mann JR, Sam M, Chu FF (2000) Low glutathione peroxidase activity in Gpx1 knockout mice protects jejunum crypts from gamma-irradiation damage. *Am J Physiol Gastrointest Liver Physiol* 279(2):G426–G436.
17. Jin RC, et al. (2011) Glutathione peroxidase-3 deficiency promotes platelet-dependent thrombosis in vivo. *Circulation* 123(18):1963–1973.
18. Fomenko DE, et al. (2009) MsrB1 (methionine-R-sulfoxide reductase 1) knock-out mice: Roles of MsrB1 in redox regulation and identification of a novel selenoprotein form. *J Biol Chem* 284(9):5986–5993.
19. Kasaikina MV, et al. (2011) Roles of the 15-kDa selenoprotein (Sep15) in redox homeostasis and cataract development revealed by the analysis of Sep 15 knockout mice. *J Biol Chem* 286(38):33203–33212.
20. Pitts MW, et al. (2013) Deletion of selenoprotein M leads to obesity without cognitive deficits. *J Biol Chem* 288(36):26121–26134.
21. Vinceti M, et al. (2014) Selenium for preventing cancer. *Cochrane Database Syst Rev* 3(3):CD005195.
22. Méplan C, Hesketh J (2014) Selenium and cancer: A story that should not be forgotten-insights from genomics. *Cancer Treat Res* 159:145–166.
23. Thuluvath PJ, Triger DR (1987) Selenium in primary biliary cirrhosis. *Lancet* 2(8552): 219.
24. Uslu N, et al. (2010) Serum selenium concentrations in cirrhotic children. *Turk J Gastroenterol* 21(2):153–155.
25. Burk RF, Early DS, Hill KE, Palmer IS, Boeglin ME (1998) Plasma selenium in patients with cirrhosis. *Hepatology* 27(3):794–798.
26. Burk RF, Hill KE, Motley AK, Byrne DW, Norsworthy BK (2015) Selenium deficiency occurs in some patients with moderate-to-severe cirrhosis and can be corrected by administration of selenate but not selenomethionine: A randomized controlled trial. *Am J Clin Nutr* 102(5):1126–1133.
27. Hatfield DL, Yoo MH, Carlson BA, Gladyshev VN (2009) Selenoproteins that function in cancer prevention and promotion. *Biochim Biophys Acta* 1790(11):1541–1545.
28. Zhuo P, Diamond AM (2009) Molecular mechanisms by which selenoproteins affect cancer risk and progression. *Biochim Biophys Acta* 1790(11):1546–1554.
29. Amsterdam A, et al. (2004) Identification of 315 genes essential for early zebrafish development. *Proc Natl Acad Sci USA* 101(35):12792–12797.
30. Howard MT, Carlson BA, Anderson CB, Hatfield DL (2013) Translational redefinition of UGA codons is regulated by selenium availability. *J Biol Chem* 288(27):19401–19413.
31. Zupanic A, Meplan C, Huguenin GV, Hesketh JE, Shanley DP (2016) Modeling and gene knockdown to assess the contribution of nonsense-mediated decay, premature termination, and selenocysteine insertion to the selenoprotein hierarchy. *RNA* 22(7): 1076–1084.
32. Novoselov SV, et al. (2007) Selenoprotein H is a nucleolar thioredoxin-like protein with a unique expression pattern. *J Biol Chem* 282(16):11960–11968.
33. Panee J, Stoytcheva ZR, Liu W, Berry MJ (2007) Selenoprotein H is a redox-sensing high mobility group family DNA-binding protein that up-regulates genes involved in glutathione synthesis and phase II detoxification. *J Biol Chem* 282(33):23759–23765.
34. Yuan M, Breitkopf SB, Yang X, Asara JM (2012) A positive/negative ion-switching, targeted mass spectrometry-based metabolomics platform for bodily fluids, cells, and fresh and fixed tissue. *Nat Protoc* 7(5):872–881.
35. Gong G, Méplan C, Gautrey H, Hall J, Hesketh JE (2012) Differential effects of selenium and knock-down of glutathione peroxidases on TNFα and flagellin inflammatory responses in gut epithelial cells. *Genes Nutr* 7(2):167–178.
36. Kipp AP, Frombach J, Deubel S, Brigelius-Flohé R (2013) Selenoprotein W as biomarker for the efficacy of selenium compounds to act as source for selenoprotein biosynthesis. *Methods Enzymol* 527:87–112.
37. Sunde RA, Raines AM, Barnes KM, Evenson JK (2009) Selenium status highly regulates selenoprotein mRNA levels for only a subset of the selenoproteins in the selenoproteome. *Biosci Rep* 29(5):329–338.
38. Kipp A, et al. (2009) Four selenoproteins, protein biosynthesis, and Wnt signalling are particularly sensitive to limited selenium intake in mouse colon. *Mol Nutr Food Res* 53(12):1561–1572.
39. Sunde RA (2010) mRNA transcripts as molecular biomarkers in medicine and nutrition. *J Nutr Biochem* 21(8):665–670.
40. Kipp AP, et al. (2012) Marginal selenium deficiency down-regulates inflammation-related genes in splenic leukocytes of the mouse. *J Nutr Biochem* 23(9):1170–1177.
41. Thisse C, et al. (2003) Spatial and temporal expression patterns of selenoprotein genes during embryogenesis in zebrafish. *Gene Expr Patterns* 3(4):525–532.
42. Kwon SY, et al. (2003) The Drosophila selenoprotein BthD is required for survival and has a role in salivary gland development. *Mol Cell Biol* 23(23):8495–8504.
43. Ben Jilani KE, Panee J, He Q, Berry MJ, Li PA (2007) Overexpression of selenoprotein H reduces Ht22 neuronal cell death after UVB irradiation by preventing superoxide formation. *Int J Biol Sci* 3(4):198–204.
44. Mendelev N, Witherspoon S, Li PA (2009) Overexpression of human selenoprotein H in neuronal cells ameliorates ultraviolet irradiation-induced damage by modulating cell signaling pathways. *Exp Neurol* 220(2):328–334.
45. Mendelev N, et al. (2011) Upregulation of human selenoprotein H in murine hippocampal neuronal cells promotes mitochondrial biogenesis and functional performance. *Mitochondrion* 11(1):76–82.
46. Mehta SL, Mendelev N, Kumari S, Andy Li P (2013) Overexpression of human selenoprotein H in neuronal cells enhances mitochondrial biogenesis and function through activation of protein kinase A, protein kinase B, and cyclic adenosine monophosphate response element-binding protein pathway. *Int J Biochem Cell Biol* 45(3):604–611.
47. Wu RT, Cao L, Chen BP, Cheng WH (2014) Selenoprotein H suppresses cellular senescence through genome maintenance and redox regulation. *J Biol Chem* 289(49): 34378–34388.
48. Zhang Y, Lu H (2009) Signaling to p53: Ribosomal proteins find their way. *Cancer Cell* 16(5):369–377.
49. Horn HF, Vousden KH (2004) Cancer: Guarding the guardian? *Nature* 427(6970): 110–111.
50. Rubbi CP, Milner J (2003) Disruption of the nucleolus mediates stabilization of p53 in response to DNA damage and other stresses. *EMBO J* 22(22):6068–6077.
51. Sasaki M, et al. (2011) Regulation of the MDM2-P53 pathway and tumor growth by PICT1 via nucleolar RPL11. *Nat Med* 17(8):944–951.
52. Bursać S, et al. (2012) Mutual protection of ribosomal proteins L5 and L11 from degradation is essential for p53 activation upon ribosomal biogenesis stress. *Proc Natl Acad Sci USA* 109(50):20467–20472.
53. Bai D, Zhang J, Xiao W, Zheng X (2014) Regulation of the HDM2-p53 pathway by ribosomal protein L6 in response to ribosomal stress. *Nucleic Acids Res* 42(3): 1799–1811.
54. Macias E, et al. (2010) An ARF-independent c-MYC-activated tumor suppression pathway mediated by ribosomal protein–Mdm2 interaction. *Cancer Cell* 18(3): 231–243.
55. Lohrum MA, Ludwig RL, Kubbutat MH, Hanlon M, Vousden KH (2003) Regulation of HDM2 activity by the ribosomal protein L11. *Cancer Cell* 3(6):577–587.
56. Zhang Y, et al. (2003) Ribosomal protein L11 negatively regulates oncoprotein MDM2 and mediates a p53-dependent ribosomal-stress checkpoint pathway. *Mol Cell Biol* 23(23):8902–8912.
57. Jin A, Itahana K, O'Keefe K, Zhang Y (2004) Inhibition of HDM2 and activation of p53 by ribosomal protein L23. *Mol Cell Biol* 24(17):7669–7680.
58. Takagi M, Absalon MJ, McLure KG, Kastan MB (2005) Regulation of p53 translation and induction after DNA damage by ribosomal protein L26 and nucleolin. *Cell* 123(1):49–63.
59. Chen J, Guo K, Kastan MB (2012) Interactions of nucleolin and ribosomal protein L26 (RPL26) in translational control of human p53 mRNA. *J Biol Chem* 287(20):16467–16476.
60. Fumagalli S, et al. (2009) Absence of nucleolar disruption after impairment of 40S ribosome biogenesis reveals an rpL11-translation-dependent mechanism of p53 induction. *Nat Cell Biol* 11(4):501–508.
61. Chen D, et al. (2007) Ribosomal protein S7 as a novel modulator of p53-MDM2 interaction: binding to MDM2, stabilization of p53 protein, and activation of p53 function. *Oncogene* 26(35):5029–5037.
62. Zhu Y, et al. (2009) Ribosomal protein S7 is both a regulator and a substrate of MDM2. *Mol Cell* 35(3):316–326.
63. Xiong X, et al. (2014) Ribosomal protein S27-like is a physiological regulator of p53 that suppresses genomic instability and tumorigenesis. *eLife* 3:e02236.
64. Kurki S, et al. (2004) Nucleolar protein NPM interacts with HDM2 and protects tumor suppressor protein p53 from HDM2-mediated degradation. *Cancer Cell* 5(5): 465–475.
65. Colombo E, Marine JC, Danovi D, Falini B, Pelicci PG (2002) Nucleophosmin regulates the stability and transcriptional activity of p53. *Nat Cell Biol* 4(7):529–533.
66. Colombo E, et al. (2005) Nucleophosmin is required for DNA integrity and p19Arf protein stability. *Mol Cell Biol* 25(20):8874–8886.
67. Li M, Gu W (2011) A critical role for noncoding 5S rRNA in regulating Mdmx stability. *Mol Cell* 43(6):1023–1032.
68. Donati G, Peddigari S, Mercer CA, Thomas G (2013) 5S ribosomal RNA is an essential component of a nascent ribosomal precursor complex that regulates the Hdm2-p53 checkpoint. *Cell Reports* 4(1):87–98.
69. Sloan KE, Bohnsack MT, Watkins NJ (2013) The 5S RNP couples p53 homeostasis to ribosome biogenesis and nucleolar stress. *Cell Reports* 5(1):237–247.
70. Uechi T, et al. (2008) Deficiency of ribosomal protein S19 during early embryogenesis leads to reduction of erythrocytes in a zebrafish model of Diamond-Blackfan anemia. *Hum Mol Genet* 17(20):3204–3211.
71. Danilova N, et al. (2014) The role of the DNA damage response in zebrafish and cellular models of Diamond Blackfan anemia. *Dis Model Mech* 7(7):895–905.
72. Heijnen HF, et al. (2014) Ribosomal protein mutations induce autophagy through S6 kinase inhibition of the insulin pathway. *PLoS Genet* 10(5):e1004371.

73. Danilova N, Sakamoto KM, Lin S (2008) Ribosomal protein S19 deficiency in zebrafish leads to developmental abnormalities and defective erythropoiesis through activation of p53 protein family. *Blood* 112(13):5228–5237.
74. Torihara H, et al. (2011) Erythropoiesis failure due to RPS19 deficiency is independent of an activated Tp53 response in a zebrafish model of Diamond-Blackfan anaemia. *Br J Haematol* 152(5):648–654.
75. Song B, et al. (2014) Systematic transcriptome analysis of the zebrafish model of Diamond-Blackfan anemia induced by RPS24 deficiency. *BMC Genomics* 15:759.
76. Mirabello L, et al. (2014) Whole-exome sequencing and functional studies identify RPS29 as a novel gene mutated in multicase Diamond-Blackfan anemia families. *Blood* 124(1):24–32.
77. Zhang Z, et al. (2013) Assessment of hematopoietic failure due to Rpl11 deficiency in a zebrafish model of Diamond-Blackfan anemia by deep sequencing. *BMC Genomics* 14:896.
78. Danilova N, Sakamoto KM, Lin S (2011) Ribosomal protein L11 mutation in zebrafish leads to haematopoietic and metabolic defects. *Br J Haematol* 152(2):217–228.
79. Chakraborty A, Uechi T, Higa S, Torihara H, Kenmochi N (2009) Loss of ribosomal protein L11 affects zebrafish embryonic development through a p53-dependent apoptotic response. *PLoS One* 4(1):e4152.
80. Zhang Y, et al. (2013) Control of hematopoietic stem cell emergence by antagonistic functions of ribosomal protein paralogs. *Dev Cell* 24(4):411–425.
81. Pereboom TC, van Weele LJ, Bondt A, MacInnes AW (2011) A zebrafish model of dyskeratosis congenita reveals hematopoietic stem cell formation failure resulting from ribosomal protein-mediated p53 stabilization. *Blood* 118(20):5458–5465.
82. Provost E, et al. (2012) Ribosomal biogenesis genes play an essential and p53-independent role in zebrafish pancreas development. *Development* 139(17):3232–3241.
83. Provost E, Weier CA, Leach SD (2013) Multiple ribosomal proteins are expressed at high levels in developing zebrafish endoderm and are required for normal exocrine pancreas development. *Zebrafish* 10(2):161–169.
84. Qin W, et al. (2014) Nom1 mediates pancreas development by regulating ribosome biogenesis in zebrafish. *PLoS One* 9(6):e100796.
85. Wang Y, Luo Y, Hong Y, Peng J, Lo L (2012) Ribosome biogenesis factor Bms1-like is essential for liver development in zebrafish. *J Genet Genomics* 39(9):451–462.
86. Zhao C, et al. (2014) Tissue specific roles for the ribosome biogenesis factor Wdr43 in zebrafish development. *PLoS Genet* 10(1):e1004074.
87. Boglev Y, et al. (2013) Autophagy induction is a Tor- and Tp53-independent cell survival response in a zebrafish model of disrupted ribosome biogenesis. *PLoS Genet* 9(2):e1003279.
88. Amsterdam A, et al. (2004) Many ribosomal protein genes are cancer genes in zebrafish. *PLoS Biol* 2(5):E139.
89. MacInnes AW, Amsterdam A, Whittaker CA, Hopkins N, Lees JA (2008) Loss of p53 synthesis in zebrafish tumors with ribosomal protein gene mutations. *Proc Natl Acad Sci USA* 105(30):10408–10413.
90. Zhang G, et al. (2010) Highly aneuploid zebrafish malignant peripheral nerve sheath tumors have genetic alterations similar to human cancers. *Proc Natl Acad Sci USA* 107(39):16940–16945.
91. Zhang G, et al. (2013) Comparative oncogenomic analysis of copy number alterations in human and zebrafish tumors enables cancer driver discovery. *PLoS Genet* 9(8): e1003734.
92. Provost E, et al. (2014) The tumor suppressor rpl36 restrains KRAS(G12V)-induced pancreatic cancer. *Zebrafish* 11(6):551–559.
93. Park EJ, et al. (2010) Dietary and genetic obesity promote liver inflammation and tumorigenesis by enhancing IL-6 and TNF expression. *Cell* 140(2):197–208.
94. Kim S, et al. (2009) Carcinoma-produced factors activate myeloid cells through TLR2 to stimulate metastasis. *Nature* 457(7225):102–106.
95. Putoczki TL, et al. (2013) Interleukin-11 is the dominant IL-6 family cytokine during gastrointestinal tumorigenesis and can be targeted therapeutically. *Cancer Cell* 24(2):257–271.
96. Marusyk A, et al. (2014) Non-cell-autonomous driving of tumour growth supports sub-clonal heterogeneity. *Nature* 514(7520):54–58.
97. Berghmans S, et al. (2005) tp53 mutant zebrafish develop malignant peripheral nerve sheath tumors. *Proc Natl Acad Sci USA* 102(2):407–412.
98. Bösl MR, Takaku K, Oshima M, Nishimura S, Taketo MM (1997) Early embryonic lethality caused by targeted disruption of the mouse selenocysteine tRNA gene (Trsp). *Proc Natl Acad Sci USA* 94(11):5531–5534.
99. Shrimali RK, et al. (2007) Selenoprotein expression is essential in endothelial cell development and cardiac muscle function. *Neuromuscul Disord* 17(2):135–142.
100. Downey CM, et al. (2009) Osteo-chondroprogenitor-specific deletion of the selenocysteine tRNA gene, Trsp, leads to chondronecrosis and abnormal skeletal development: a putative model for Kashin-Beck disease. *PLoS Genet* 5(8):e1000616.
101. Sengupta A, et al. (2010) Selenoproteins are essential for proper keratinocyte function and skin development. *PLoS One* 5(8):e12249.
102. Wirth EK, et al. (2010) Neuronal selenoprotein expression is required for interneuron development and prevents seizures and neurodegeneration. *FASEB J* 24(3):844–852.
103. Wirth EK, et al. (2014) Cerebellar hypoplasia in mice lacking selenoprotein biosynthesis in neurons. *Biol Trace Elem Res* 158(2):203–210.
104. Carlson BA, et al. (2004) Specific excision of the selenocysteine tRNA[Ser]Sec (Trsp) gene in mouse liver demonstrates an essential role of selenoproteins in liver function. *J Biol Chem* 279(9):8011–8017.
105. Kasaikina MV, et al. (2013) Contrasting roles of dietary selenium and selenoproteins in chemically induced hepatocarcinogenesis. *Carcinogenesis* 34(5):1089–1095.
106. Sengupta A, et al. (2008) A functional link between housekeeping selenoproteins and phase II enzymes. *Biochem J* 413(1):151–161.
107. Kawatani Y, Suzuki T, Shimizu R, Kelly VP, Yamamoto M (2011) Nrf2 and selenoproteins are essential for maintaining oxidative homeostasis in erythrocytes and protecting against hemolytic anemia. *Blood* 117(3):986–996.
108. Suzuki T, et al. (2008) Deletion of the selenocysteine tRNA gene in macrophages and liver results in compensatory gene induction of cytoprotective enzymes by Nrf2. *J Biol Chem* 283(4):2021–2030.
109. Luchman HA, Villemaire ML, Bismar TA, Carlson BA, Jirik FR (2014) Prostate epithelium-specific deletion of the selenocysteine tRNA gene Trsp leads to early onset intraepithelial neoplasia. *Am J Pathol* 184(3):871–877.
110. Diwadkar-Navsariwala V, et al. (2006) Selenoprotein deficiency accelerates prostate carcinogenesis in a transgenic model. *Proc Natl Acad Sci USA* 103(21):8179–8184.
111. Hudson TS, et al. (2012) Selenoproteins reduce susceptibility to DMBA-induced mammary carcinogenesis. *Carcinogenesis* 33(6):1225–1230.
112. Chu FF, et al. (2004) Bacteria-induced intestinal cancer in mice with disrupted Gpx1 and Gpx2 genes. *Cancer Res* 64(3):962–968.
113. Esworthy RS, et al. (2001) Mice with combined disruption of Gpx1 and Gpx2 genes have colitis. *Am J Physiol Gastrointest Liver Physiol* 281(3):G848–G855.
114. Brigelius-Flohé R, Kipp AP (2012) Physiological functions of GPx2 and its role in inflammation-triggered carcinogenesis. *Ann N Y Acad Sci* 1259:19–25.
115. Krehl S, et al. (2012) Glutathione peroxidase-2 and selenium decreased inflammation and tumors in a mouse model of inflammation-associated carcinogenesis whereas sulforaphane effects differed with selenium supply. *Carcinogenesis* 33(3):620–628.
116. Banning A, et al. (2008) Glutathione peroxidase 2 inhibits cyclooxygenase-2-mediated migration and invasion of HT-29 adenocarcinoma cells but supports their growth as tumors in nude mice. *Cancer Res* 68(23):9746–9753.
117. Emmink BL, et al. (2014) GPx2 suppression of H_2O_2 stress links the formation of differentiated tumor mass to metastatic capacity in colorectal cancer. *Cancer Res* 74(22):6717–6730.
118. Irons R, Carlson BA, Hatfield DL, Davis CD (2006) Both selenoproteins and low molecular weight selenocompounds reduce colon cancer risk in mice with genetically impaired selenoprotein expression. *J Nutr* 136(5):1311–1317.
119. Novoselov SV, et al. (2005) Selenoprotein deficiency and high levels of selenium compounds can effectively inhibit hepatocarcinogenesis in transgenic mice. *Oncogene* 24(54):8003–8011.
120. Her GM, Yeh YH, Wu JL (2003) 435-bp liver regulatory sequence in the liver fatty acid binding protein (L-FABP) gene is sufficient to modulate liver regional expression in transgenic zebrafish. *Dev Dyn* 227(3):347–356.
121. Goessling W, et al. (2008) APC mutant zebrafish uncover a changing temporal requirement for wnt signaling in liver development. *Dev Biol* 320(1):161–174.
122. Farooq M, et al. (2008) Histone deacetylase 3 (hdac3) is specifically required for liver development in zebrafish. *Dev Biol* 317(1):336–353.
123. Holtzinger A, Evans T (2005) Gata4 regulates the formation of multiple organs. *Development* 132(17):4005–4014.
124. Weber M, Mickoleit M, Huisken J (2014) Light sheet microscopy. *Methods Cell Biol* 123:193–215.
125. Collins JE, White S, Searle SM, Stemple DL (2012) Incorporating RNA-seq data into the zebrafish Ensembl genebuild. *Genome Res* 22(10):2067–2078.
126. Luo W, Friedman MS, Shedden K, Hankenson KD, Woolf PJ (2009) GAGE: Generally applicable gene set enrichment for pathway analysis. *BMC Bioinformatics* 10:161.
127. Dickinson BC, Huynh C, Chang CJ (2010) A palette of fluorescent probes with varying emission colors for imaging hydrogen peroxide signaling in living cells. *J Am Chem Soc* 132(16):5906–5915.
128. Lee BC, Le DT, Gladyshev VN (2008) Mammals reduce methionine-S-sulfoxide with MsrA and are unable to reduce methionine-R-sulfoxide, and this function can be restored with a yeast reductase. *J Biol Chem* 283(42):28361–28369.
129. Spitsbergen JM, et al. (2000) Neoplasia in zebrafish (Danio rerio) treated with 7,12-dimethylbenz[a]anthracene by two exposure routes at different developmental stages. *Toxicol Pathol* 28(5):705–715.
130. Cox AG, et al. (2016) Yap reprograms glutamine metabolism to increase nucleotide biosynthesis and enable liver growth. *Nat Cell Biol* 18(8):886–896.
131. Chen J, et al. (2005) Loss of function of def selectively up-regulates Delta113p53 expression to arrest expansion growth of digestive organs in zebrafish. *Genes Dev* 19(23):2900–2911.
132. Li Y, et al. (2014) Inflammatory signaling regulates embryonic hematopoietic stem and progenitor cell production. *Genes Dev* 28(23):2597–2612.
133. Fang Y, et al. (2013) Translational profiling of cardiomyocytes identifies an early Jak1/Stat3 injury response required for zebrafish heart regeneration. *Proc Natl Acad Sci USA* 110(33):13416–13421.
134. Jeffery J, et al. (2015) Cep55 regulates embryonic growth and development by promoting Akt stability in zebrafish. *FASEB J* 29(5):1999–2009.